Variability of Shallow and Deep Western Boundary Currents off the Bahamas during 2004–05: Results from the 26°N RAPID–MOC Array

W. E. JOHNS AND L. M. BEAL

Division of Meteorology and Physical Oceanography, Rosenstiel School of Marine and Atmospheric Science, University of Miami, Miami, Florida

M. O. BARINGER

Physical Oceanography Division, NOAA/Atlantic Oceanographic and Meteorological Laboratory, Miami, Florida

J. R. MOLINA

Division of Meteorology and Physical Oceanography, Rosenstiel School of Marine and Atmospheric Science, University of Miami, Miami, Florida

S. A. CUNNINGHAM, T. KANZOW, AND D. RAYNER

Ocean Observing and Climate Research Group, National Oceanography Centre, Southampton, Southampton, United Kingdom

(Manuscript received 2 March 2007, in final form 17 July 2007)

ABSTRACT

Data from an array of six moorings deployed east of Abaco, Bahamas, along 26.5°N during March 2004–May 2005 are analyzed. These moorings formed the western boundary array of a transbasin observing system designed to continuously monitor the meridional overturning circulation and meridional heat flux in the subtropical North Atlantic, under the framework of the joint U.K.–U.S. Rapid Climate Change (RAPID)–Meridional Overturning Circulation (MOC) Program. Important features of the western boundary circulation include the southward-flowing deep western boundary current (DWBC) below 1000 m and the northward-flowing "Antilles" Current in the upper 1000 m. Transports in the western boundary layer are estimated from direct current meter observations and from dynamic height moorings that measure the spatially integrated geostrophic flow between moorings. The results of these methods are combined to estimate the time-varying transports in the upper and deep ocean over the width of the western boundary layer to a distance of 500 km offshore of the Bahamas escarpment. The net southward transport of the DWBC across this region, inclusive of northward deep recirculation, is −26.5 Sv (Sv $\equiv 10^6$ m^3 s^{-1}), which is divided nearly equally between upper (−13.9 Sv) and lower (−12.6 Sv) North Atlantic Deep Water (NADW). In the top 1000 m, 6.0 Sv flows northward in a thermocline-intensified jet near the western boundary. These transports are found to agree well with historical current meter data in the region collected between 1986 and 1997. Variability in both shallow and deep components of the circulation is large, with transports above 1000 m varying between −15 and +25 Sv and deep transports varying between −60 and +3 Sv. Much of this transport variability, associated with barotropic fluctuations, occurs on relatively short time scales of several days to a few weeks. Upon removal of the barotropic fluctuations, slower baroclinic transport variations are revealed, including a temporary stoppage of the lower NADW transport in the DWBC during November 2004.

1. Introduction

Western boundary currents in the subtropical North Atlantic Ocean play an important role in both the wind-driven and large-scale thermohaline circulation. The deep western boundary current (DWBC) originates from dense overflows in the Greenland/Norwegian Seas and deep convection in the subpolar gyre, and carries these cold waters southward throughout the basin along the western boundary (Schmitz and McCartney 1993). In compensation for this deep southward flow, warm waters flow northward in the upper ocean, leading to a northward oceanic heat flux that peaks at

Corresponding author address: W. Johns, Division of Meteorology and Physical Oceanography, Rosenstiel School of Marine and Atmospheric Science, University of Miami, Miami, FL 33149.
E-mail: bjohns@rsmas.miami.edu

DOI: 10.1175/2007JPO3791.1

greater than 1.0 PW near 25°N (Hall and Bryden 1982). Much of this northward flow is carried in the Gulf Stream within the Straits of Florida or in shallow western boundary currents east of the Bahamas. The system of shallow and deep currents making up this large-scale thermohaline circulation, combined with wind-driven transports in the surface Ekman layer, is referred to as the meridional overturning circulation (MOC).

Estimates of the strength of the Atlantic MOC and associated heat transport have typically been made from transbasin hydrographic sections along one latitude combined with direct measurements of the western boundary currents (Hall and Bryden 1982; Bryden et al. 2005) or from sections at several different latitudes in an inverse calculation (Ganachaud and Wunsch 2000; Lumpkin and Speer 2003). These approaches require a number of assumptions, including temporal stationarity of the hydrographic fields and currents, which may or may not be accurate. A new approach to the problem of measuring the MOC is to make continuous observations of the currents and hydrographic fields with long-term moorings or other time series techniques, so as to obtain a temporal mean value for the MOC as well as information on its time scales and range of variability. The first attempt to instrument a complete transbasin section for this purpose is now in place along 26°N in the Atlantic as part of the joint U.K.–U.S. Rapid Climate Change (RAPID)–MOC Program (Cunningham et al. 2007). The 26°N RAPID–MOC array is a collaboration between scientists at the U.K. National Oceanography Centre, Southampton, under the U.K RAPID program, and scientists at the University of Miami and NOAA's Atlantic Oceanographic and Meteorological Laboratory under the U.S. Meridional Overturning Circulation and Heat Flux Array (MOCHA) program.

The overall strategy for RAPID–MOC consists of the deployment of deep-water endpoint "dynamic height" moorings on either side of the basin to monitor the basinwide geostrophic shear, combined with observations from clusters of moorings up the western (Bahamas) and eastern (African) continental margins, and direct measurements of the flow though the Straits of Florida. Moorings are also included on the flanks of the Mid-Atlantic Ridge to resolve flows in either subbasin. Ekman transports derived from satellite winds are then combined with the geostrophic and direct current observations and an overall mass conservation constraint to continuously estimate the basinwide MOC strength and vertical structure. Precision bottom pressure gauges are also employed to monitor absolute transports, including barotropic circulation. The overall methodology is described in more detail in Kanzow et al. (2007), where it is applied to the first year results from the 26°N array to estimate the Atlantic MOC strength and variability during 2004–05 (see also Cunningham et al. 2007).

In this paper we present the results from the first setting of moorings off the Bahamas that make up the critical western boundary part of the 26°N array. The specific role of these observations in the overall MOC calculation is the determination of the time-varying transport (magnitude and vertical structure) in the region shoreward of the deep water dynamic-height mooring making up the western "endpoint" of the section. However, it is also of interest to determine the transports over the full width of the western boundary layer, which extends farther offshore, including the net transport of the DWBC and the overlying shallow "Antilles" Current, as these currents are important individual components of the MOC. Here we use the western boundary array measurements to estimate the mean transport and variability of the DWBC and Antilles Current for the period from March 2004 to May 2005, and describe in detail the techniques used to produce the western boundary transports required for the basinwide MOC calculation (Cunningham et al. 2007). Transports computed over an extended western boundary layer (to 500 km offshore of Abaco, Bahamas) are in good agreement with earlier estimates based on the decade-long World Ocean Circulation Experiment (WOCE) Atlantic Current Meter (ACM-1) line at the same location (Lee et al. 1996; Bryden et al. 2005), suggesting that the western boundary transports during the first year of the RAPID–MOC experiment were fairly typical of mean conditions. However, the observations reveal interesting aspects of the variability of the DWBC that had not been resolved before, including large changes in the internal (baroclinic) structure of the DWBC.

2. Observations

a. Moored time series measurements

The primary data used in this analysis are time series records from current meters, temperature/salinity recorders, and precision bottom pressure gauges deployed on taut-wire subsurface moorings east of Abaco, Bahamas. The moorings were deployed from the RRS *Discovery* in late March 2004 and recovered on the R/V *Knorr* in early May 2005. All moorings were nominally along 26.5°N latitude, with some small deviations owing to topographic irregularities (Figs. 1a and 2). The array consisted of a closely spaced cluster of four moorings (denoted WBA–WB2) over the steep continental slope and rise of the Bahamas escarpment, a pair of moorings

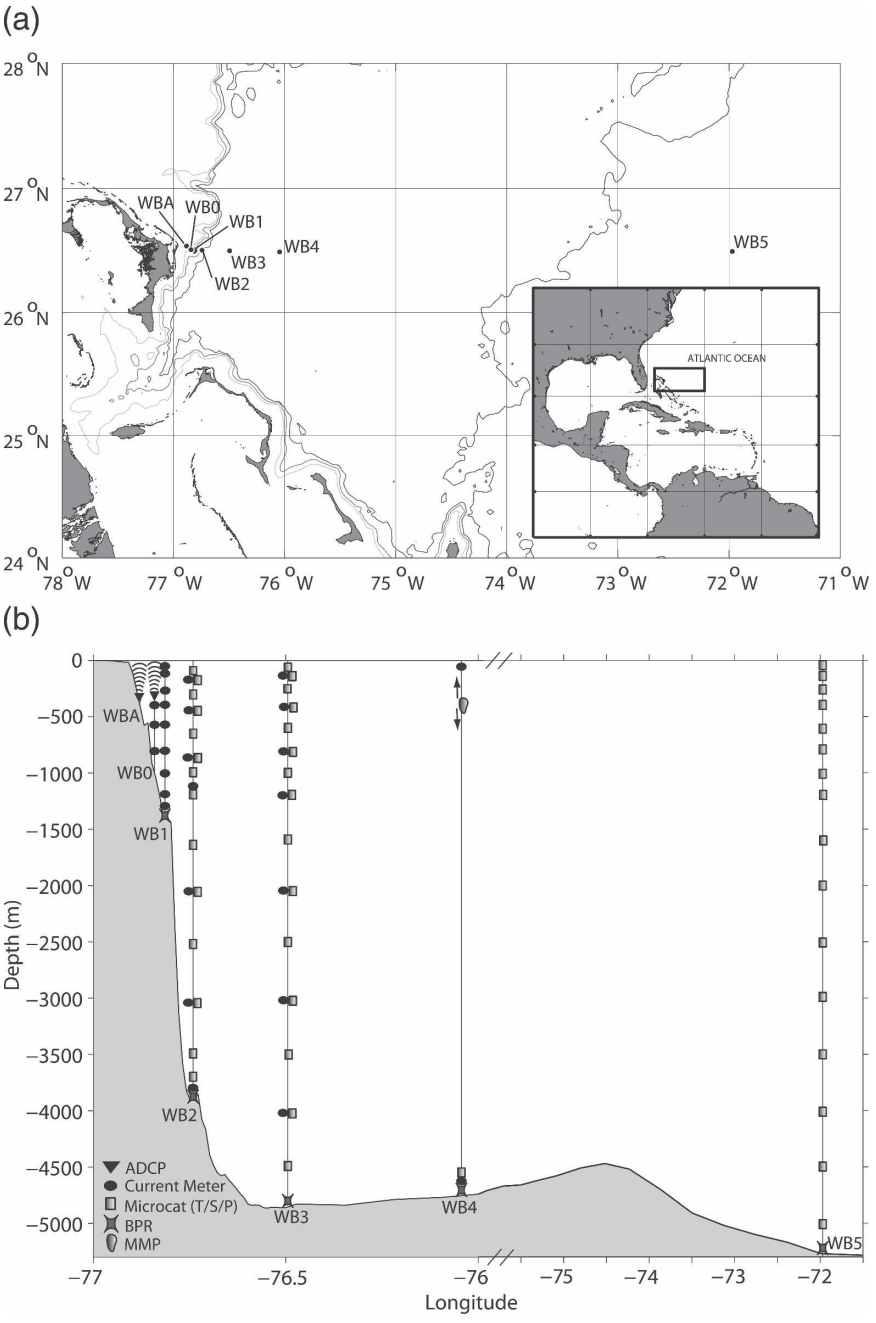

FIG. 1. (a) The RAPID–MOC western boundary array: Moorings WBA–WB4 compose a tightly spaced array near the Bahamas escarpment, while mooring WB5 lies 500 km offshore and forms a "dynamic height" endpoint for the array. (b) Cross-sectional view of the array over topography, showing the instrument types and depths on the moorings. (Note the expanded distance scale near the western boundary, west of 76°W.) Little data were recovered from the moored profiler (MMP) on WB4, and no data from WB4 were used in the analysis.

spanning the usual domain of the DWBC within 100 km of the western boundary (WB3 and WB4), and a final mooring deployed approximately 500 km offshore at 72°W (WB5). Instrument configuration on the moorings is shown in Fig. 1b.

1) CURRENT MEASUREMENTS

Current meters were included on the five westernmost moorings (WBA–WB3) and consisted of a mix of Aanderaa RCM-11s, Nortek Aquadopps, Interocean

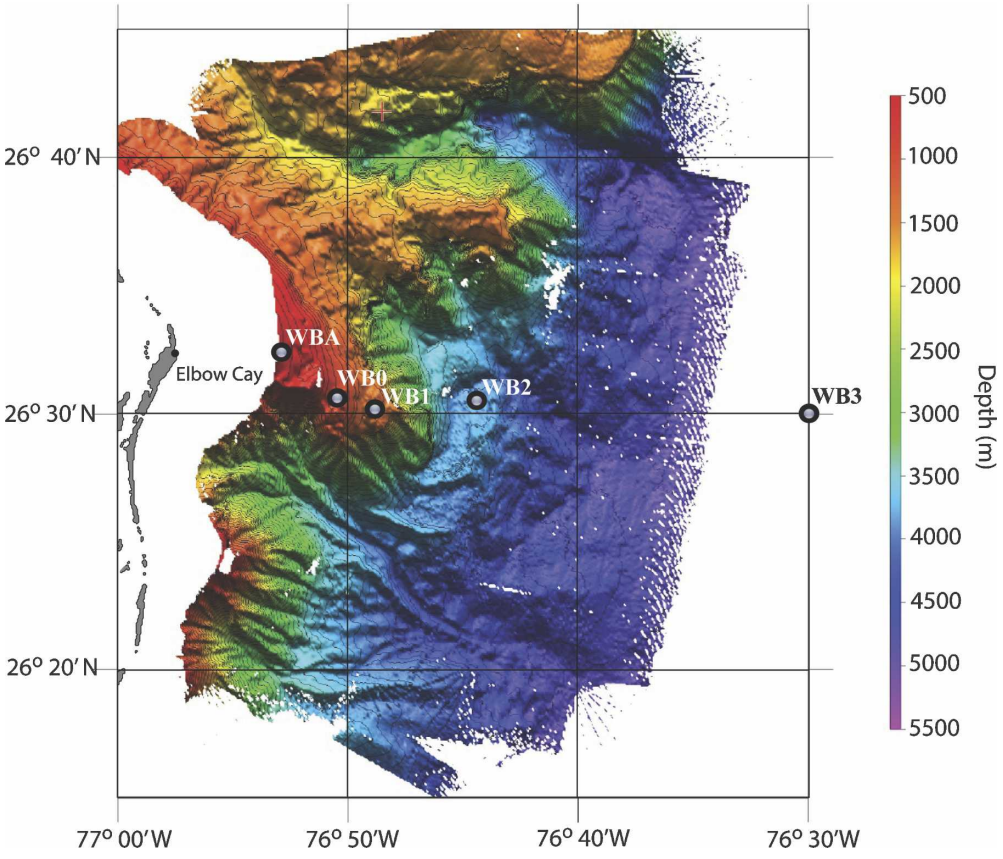

FIG. 2. Bathymetry of the Bahamas escarpment off Elbow Cay, Abaco, Bahamas, derived from a multibeam (Seabeam) acoustic bottom survey on the R/V *Ronald H. Brown* in June 2002. The mooring sites in the western boundary array cluster from WBA to WB3 are indicated.

S4s, and Sontek Argonauts. Two R.D. Instruments acoustic Doppler current profilers (ADCPs) were also deployed on the moorings at sites WBA (broadband 150 kHz, near bottom) and WB0 (narrowband 150 kHz, atop the mooring). Mooring WB4 had a McClane Moored Profiler (MMP) with an acoustic current meter that was intended to cycle between 75 and 4500 m, but the MMP failed to cycle after a short time and therefore its limited data (currents and temperature/salinity) are not used in the following analysis. All current meters measured vector-averaged currents with recording intervals from 15 min to 1 h.

Time series of the vector currents at each mooring site are shown in Figs. 3a–e, after low-pass filtering with a 40-h Butterworth filter to remove tidal and inertial oscillations (which are the processed currents used in all subsequent analysis). The overall data recovery for the current measurements was 88%, with the largest problems occurring on WB2 where there were a number of short records owing to battery failures or other causes and at WBA where the mooring released prematurely from the bottom. Apart from these problems the data were of very high quality. Nearly all of the current meters were equipped with strain gauge pressure sensors to keep track of mooring motion, and therefore the depths of each instrument are known at all times.

2) TEMPERATURE/SALINITY MEASUREMENTS

All current meters on mooring WB1 (RCM-11s and S4s) were equipped with conductivity cells, and thus provide temperature and salinity measurements in addition to currents at each level. Higher-precision Seabird 37 (MicroCat) temperature/conductivity/pressure recorders were included on moorings WB2–WB5 at each current measurement level and at additional levels throughout the water column to provide high-quality measurements of the time-varying temperature and salinity profiles at these sites. These moorings are intended to function as "standing CTDs" that allow monitoring of the varying dynamic height profile at each site for inference of geostrophic currents.

To ensure maximum accuracy in the temperature and salinity measurements, a special calibration procedure

is followed in which each instrument, before deployment and after recovery, is attached to a shipboard CTD package and lowered through its design pressure range with numerous (5 min long) bottle stops on retrieval. This procedure provides a highly accurate in situ calibration that is then applied to the data from each deployment (Kanzow et al. 2006). Estimated final accuracies for the SBE 37 measurements are 0.005°C for temperature, 0.01 for salinity, and 4 dbar for pressure. The methodology used to convert these discrete temperature and salinity measurements into continuous vertical profiles and associated uncertainties are discussed in the following section. An example is shown in Fig. 4 where the potential temperature profile variability at sites WB2 and WB3 is displayed.

Site WB2 is intended to serve as the western boundary "endpoint" dynamic height mooring for the transbasin section and is therefore placed as close to the escarpment as practicable while still being in relatively deep water. Mooring WB3 serves as a backup dynamic height mooring for WB2 and also provides direct velocity measurements near the mean core of the DWBC. Mooring WB4 was placed near the offshore edge of the DWBC and was intended (with WB2) to provide integrated geostrophic transport estimates across the typical domain of the DWBC. Finally, mooring WB5 was placed well offshore of the western boundary to capture transport variability associated with offshore meandering of the DWBC and localized recirculation cells adjacent to the western boundary.

3) BOTTOM PRESSURE MEASUREMENTS

Precision bottom pressure measurements were obtained at the base of all dynamic height moorings (WB1, WB2, WB3, and WB5) using SeaBird SBE 16 plus or SBE 53 bottom pressure recorders (BPRs) equipped with Digiquartz pressure sensors. The purpose of these measurements is to determine the time-varying reference velocity for geostrophic currents from the dynamic height moorings (see next section). The resolution of the pressure measurements is 0.001 dbar (equivalent to 1 mm) for the sampling setup used. (n.b. the absolute accuracy of the bottom pressures is 0.01% of full scale, or approximately 0.7 dbar for the 10 000 psi gauges used in this experiment, much too large to determine absolute pressure gradients associated with oceanic flows.) Additionally, there can be substantial long-term drift of the bottom pressure sensors of up to several tenths of a decibar that requires estimation and removal (Watts and Kontoyiannis 1990).

The bottom pressure records from sites WB2, WB3, and WB5, after removal of their mean values and the daily/semidaily tides, are shown in Fig. 5, before and after drift removal. Drifts were removed from each sensor using a least squares exponential–linear fit (Watts and Kontoyiannis 1990; see also Johns et al. 2005, hereafter J05). The drift curves for the instruments were fairly typical of our past experience with these instruments, with overall record-length drifts on the order of 0.2 dbar.

b. *Shipboard observations*

Three cruises were conducted during the time period of the array observations: (i) 4 April–10 May 2004 (RRS *Discovery*), (ii) 22 September–3 October 2004 (R/V *Ronald H. Brown*), and (iii) 2–26 May 2005 (R/V *Knorr*, array servicing). On each cruise a set of serial stations were occupied along 26.5°N east of Abaco from the western boundary to at least 72°W (the location of WB5). The station spacing ranged from approximately 8 km close to the western boundary to 50 km at the offshore end of the line, gradually increasing in the offshore direction. Conventional conductivity/temperature/depth/dissolved oxygen ($CTDO_2$) profiles were acquired using a SeaBird SBE-911plus pumped system and direct velocity profiles were measured using a dual-ADCP system mounted on the $CTDO_2$ package [lowered ADCP (LADCP)]. Calibration of the $CTDO_2$ data was performed using salinity and dissolved oxygen bottle samples drawn from a 24-bottle Rosette, with accuracies of 0.001 for temperature, 0.003 for salinity, and 2.0 dbar for pressure. The calibrated temperature and conductivity data were used for final calibrations of the moored CTD sensors as previously described.

The LADCP system used on all cruises was a dual-frequency "hybrid" system consisting of a downward-looking 150-kHz broadband ADCP and an upward-looking 300-kHz Workhorse ADCP. The data were processed with Visbeck/Lamont-Doherty Earth Observatory (LDEO) version 9 software (Visbeck 2002), which incorporates CTD pressure data to constrain the profile vertical mapping, as well as absolute bottom-track velocity data and upper-ocean shipboard ADCP velocity data to constrain the overall velocity profile. The accuracy of LADCP velocity profiles is estimated to be approximately 5 cm s^{-1}, with lower errors for the vertically integrated (barotropic) velocity (Hacker et al. 1996). Here, we will use the LADCP data for comparison with the velocity structure derived from the moored array and to help "level" the bottom pressure records to obtain absolute transports from the dynamic height moorings (see following section).

Shipboard ADCP systems were continuously operated on each cruise to measure the upper-ocean cur-

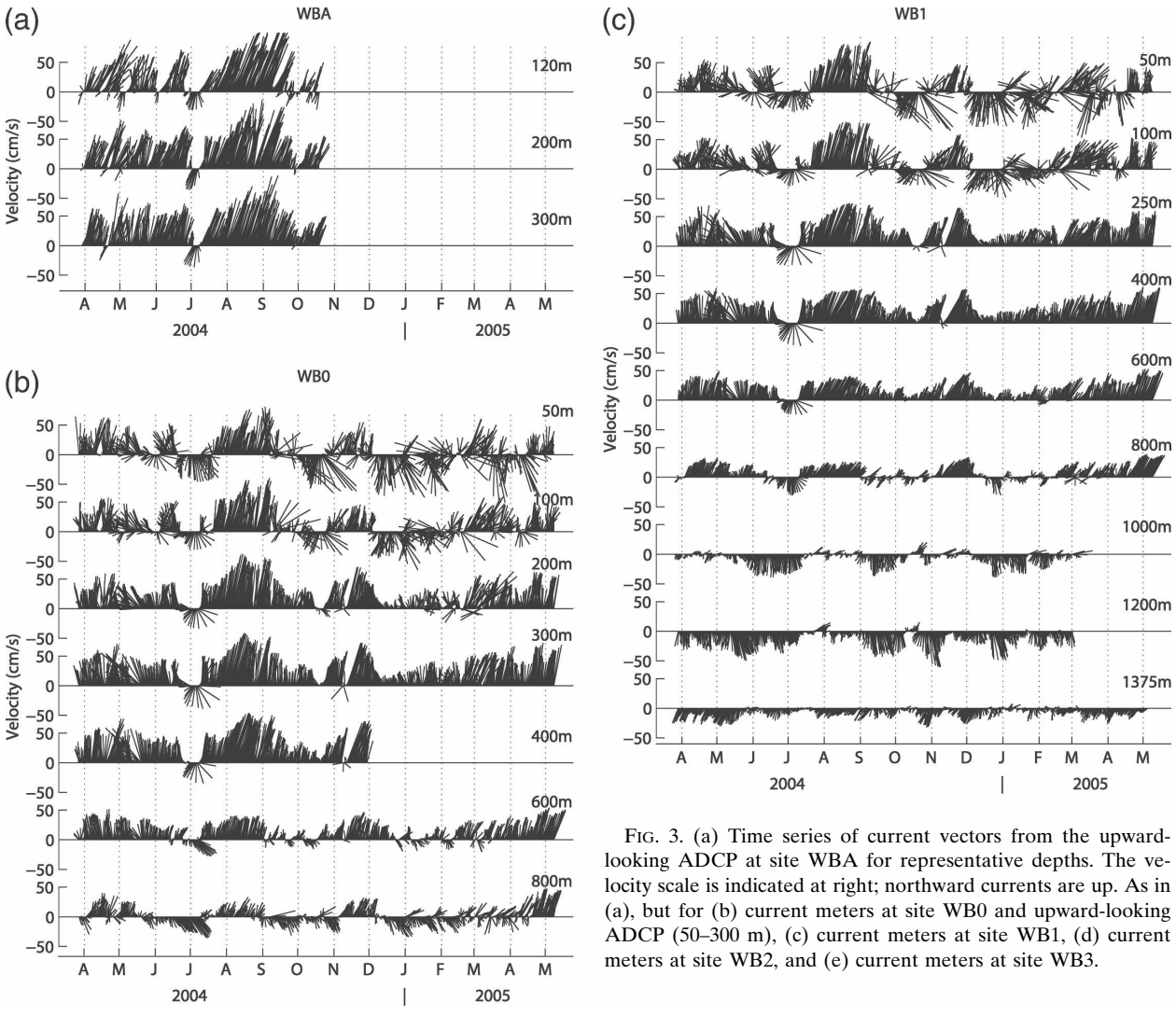

FIG. 3. (a) Time series of current vectors from the upward-looking ADCP at site WBA for representative depths. The velocity scale is indicated at right; northward currents are up. As in (a), but for (b) current meters at site WB0 and upward-looking ADCP (50–300 m), (c) current meters at site WB1, (d) current meters at site WB2, and (e) current meters at site WB3.

rents. The ADCP systems and their nominal vertical ranges of good data during the cruises were (i) March 2004 (RRS *Discovery*): dual system, 75/150 kHz, 780 m; (ii) September–October 2004 (R/V *Ronald H. Brown*): single system, 150 kHz, 270 m; and (iii) May 2005 (R/V *Knorr*): dual system, 75/150 kHz, 760 m. In addition to the use of on-station data to constrain the simultaneous LADCP profiles, the continuous along-section data from the shipboard ADCPs were merged with the LADCP station data to provide improved velocity structure and transport estimates in the upper ocean.

3. Methods: Transport estimates

a. Direct transports from current meters

A time series of transport for the region shoreward of WB3 can be derived from the direct current meter measurements. The procedure for computing these transports follows the same approach used for the previous ACM-1 current meter arrays in this region (e.g., Lee et al. 1996). First, the current measurements at each mooring site are interpolated vertically using a shape-preserving cubic spline (Akima 1970), with extension of the velocity profile to the surface using constant shear above the top instrument and to the bottom with constant velocity from the deepest instrument. The vertical current profiles at each site are then linearly interpolated in the horizontal between the moorings and to the boundaries of the sloping topography. The resulting interpolated field is computed every 12 h from the low-pass-filtered data and saved on a 20 m (vertical) by 2 km (horizontal) cross-sectional grid. Transports in various layers or for various horizontal distances from the western boundary can then be easily computed by sum-

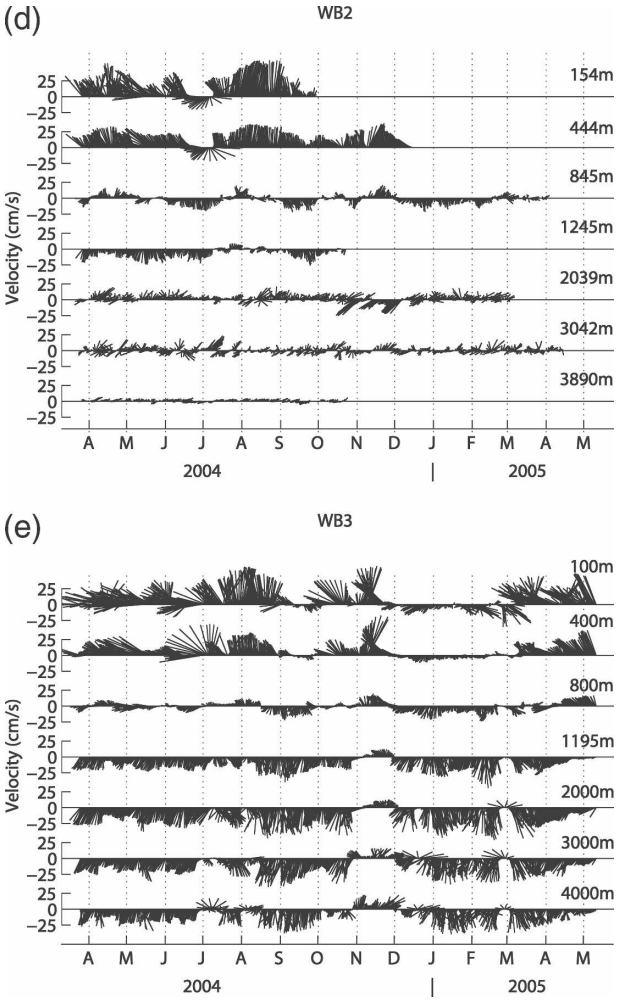

FIG. 3. (*Continued*)

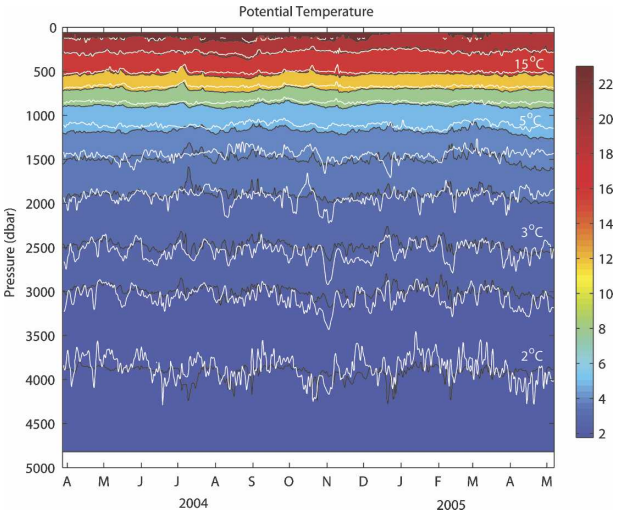

FIG. 4. Time series of potential temperature vs depth at mooring site WB3 (in colors and black contours), derived from the temperature/salinity recorders on the mooring. White contours show the respective potential temperatures at nearby mooring WB2. Potential temperature surfaces contoured are (from bottom to top) 2.0°, 2.5°, 3.0°, 3.5°, 4.0°, 5.0°, 8.0°, 12.0°, 15.0°, 19.0°, and 23.0°C.

ming over respective parts of the grid. The mean currents over the length of the deployment derived from this procedure are shown in Fig. 6.

To extend the time series over the full length of the deployment period, a method has to be devised to fill in for the current meter records that stopped prematurely. Linear regressions with nearby current meter records either on the same mooring or adjacent moorings, which explained high levels of variance of the available parts of these records, were used to extend several of the records, including WBA, WB0 (400 m), WB1 (1000 and 1200 m), and parts of WB2 (150 and 1250 m). Mooring WB2 was most problematic in this regard due to a number of separate failures, and it was not possible to reasonably extend the full vertical profile of currents on that mooring past mid-December 2004. Therefore, after 15 December 2004, no current data are used from WB2 in the interpolation and gridding procedure. For the upper-ocean currents this simply means that linear interpolation is carried straight across between moorings WB1 and WB3, but for the deep currents a problem is created in how to extrapolate deep currents from WB3 to the escarpment. As can be seen in Fig. 6 (and also in Fig. 3d) the deep currents on WB2 are weak and show a strong signature of "shielding" by the escarpment. This is caused by upstream ridges protruding from the escarpment with ridge crests at about 1600 m, as can be seen in Fig. 2 near 26°38′N and 26°44′N. (This

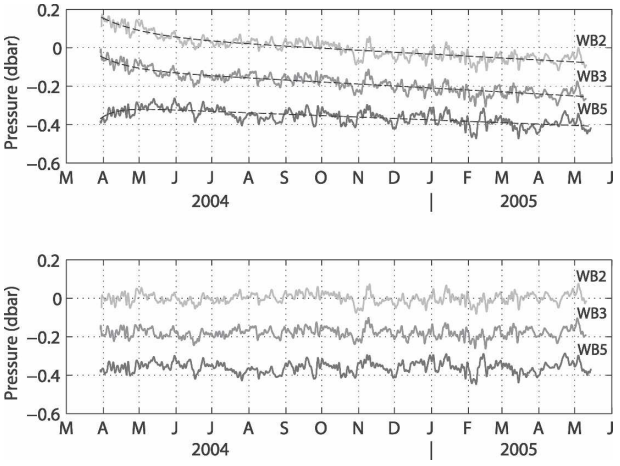

FIG. 5. Detided bottom pressure time series (top) from sites WB2, WB3, and WB5, and (bottom) after detrending with an exponential–linear fit. The series are offset by an arbitrary amount (0.2 dbar) for display purposes; each time series has had its mean absolute value removed.

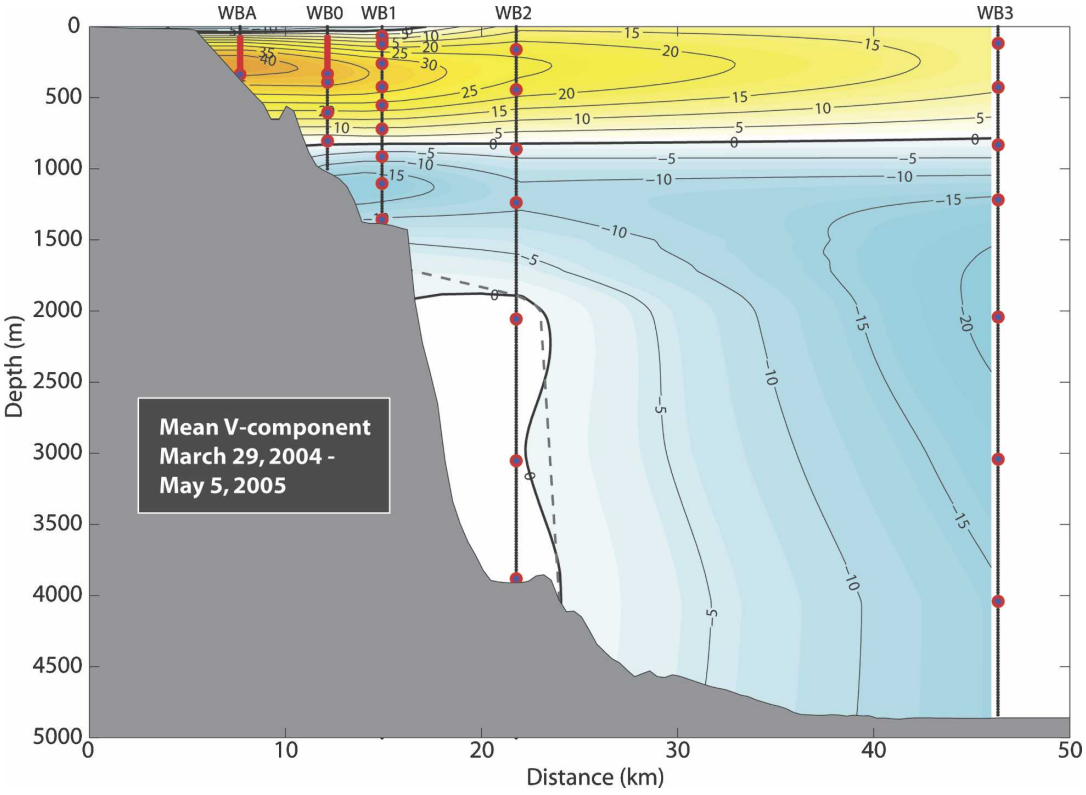

FIG. 6. Mean northward velocity from the gridded current meter data shoreward of WB3. The red dots and lines (for ADCPs) show the measurement locations. The bold dashed line shows the topography mask used to simulate the deep shielded zone inside of mooring WB2 during the latter part of the moored transport calculation (after mid-December 2004). Velocity contours: cm s^{-1}.

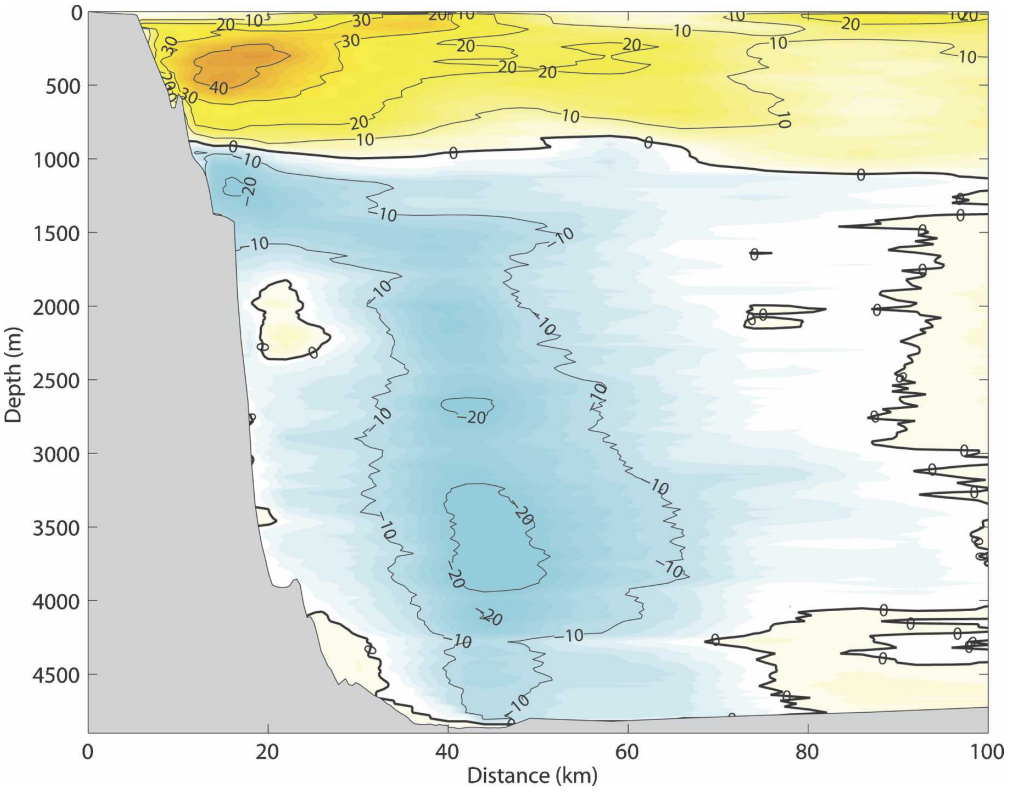

FIG. 7. Average northward velocity derived from the mean of the three LADCP sections acquired during the period of the moored observations (during April 2005, September 2004, and May 2005, respectively).

effect was known in advance from previous current measurements off Abaco, but WB2 was deliberately placed here to keep it inshore of the DWBC.) To mimic the effect of this shielded zone after mid-December 2004, a fake wall is introduced, as shown in Fig. 6, along which the velocity is set to zero before interpolation. We will show later that this leads to consistent transport estimates between the early and later parts of the record.

b. *Indirect transports from dynamic height moorings*

Geostrophic transports derived from dynamic height moorings have been used successfully in a number of field experiments (Whitworth 1983; Johns et al. 2001; J05; Kanzow et al. 2006). For a detailed description of methods and errors the reader is referred to J05 or Kanzow et al. (2006). Briefly, the following steps are required:

1) The discrete temperature and salinity measurements at known pressures on the moorings are interpolated vertically to produce continuous profiles;
2) Dynamic height profiles are calculated for each mooring and differenced to produce profiles of the spatially averaged geostrophic velocity between adjacent moorings, relative to an (unknown) reference value;
3) Bottom pressure data from the moorings are differenced to produce an estimate of the *time variability* of the near-bottom reference velocity;
4) A remaining constant (the time-mean value of the reference velocity) is estimated from other observations (e.g., LADCP) in order to derive absolute transports.

The methodology used for step 1 follows that of Fillenbaum et al. (1997) and J05 for the same region of study. An empirical function representing the climatological vertical temperature gradient as a function of temperature, $dT/dz(T)$, derived from historical CTD data, is used to interpolate the temperature profile vertically between the measurement levels on a 20-m grid. A similar approach is used for the salinity profile based on the climatological $dS/dz(T)$ field once the temperature profile is created. The resulting temperature and salinity profiles connect through all discrete temperature and salinity measurement points on the mooring, but are otherwise consistent with the climatological vertical temperature structure and T/S relation for the region. In tests against real CTD profiles this approach has been shown to be superior to other methods (J05). The typical error in dynamic height (geopotential) at the surface relative to a deep reference level using this method is approximately 2 dyn cm (0.2 m^2 s^{-2}), and the resulting cumulative baroclinic transport error, relative to the bottom, is ± 2 Sv (Sv $\equiv 10^6$ m^3 s^{-1}). The error does not depend on mooring separation; it is the same for widely or closely spaced moorings. We refer to the resulting transport-per-unit-depth profile between moorings (i.e., the spatially averaged velocity times the mooring separation) as the *baroclinic transport profile*, V_{bc}.

Bottom pressure records, processed as described previously, are used to estimate the time-varying reference velocity between moorings relative to an unknown constant. In terms of the transport per unit depth at the reference level,

$$V'_{ref}(t) = (\rho f)^{-1}[p_2(t) - p_1(t)],$$

where p_2 and p_1 are the bottom pressure variations at the two sites. If the two moorings are in different depths, then the reference level is chosen as the greatest common depth of the two moorings. The deeper bottom pressure record must also then be corrected to that reference level by subtracting any contribution to the bottom pressure from the time-varying dynamic height between the bottom and the reference level (a process we refer to as "hydroadjusting"). Random transport errors related to the uncertainty in bottom pressure measurements are approximately ± 1.5 Sv (J05).

Adding this time-varying reference value to the baroclinic transport profile yields the total transport profile $V'(t) = V_{bc}(t) + V'_{ref}(t)$ relative to an unknown constant, V_0, the time mean transport per unit depth at the reference level. In principle, this constant can be determined by one-time direct velocity measurements at the reference level in the region between the moorings; in practice, it is necessary to have several such estimates for redundancy (J05). If only the transport *variability* is of interest, this is unnecessary. Here we use the combined shipboard and lowered-ADCP data from the three cruises to determine the reference value. Following J05, we use the full water column absolute velocity data from shipboard and lowered ADCP to constrain the estimates of V_0 rather than just the velocity measured at the reference level, which reduces the overall noise in the V_0 estimates. Once the value of V_0 is specified, the time-varying absolute transport profile $V(t) = V_{bc}(t) + [V'_{ref}(t) + V_0]$ is determined.

4. Results

a. *Transports and velocity structure in the inner western boundary region*

The current meter measurements were designed to provide a well-resolved picture of the flow distribution

and its variability inshore of mooring WB2 and corresponding direct transport estimates for this region. Contributions to the meridional flow in this region have to be combined with geostrophic interior transports derived from dynamic height moorings (at WB2, and similarly at the eastern boundary) to determine the net interior flow (Kanzow et al. 2007). Alternatively, WB3 could serve as a western boundary dynamic height endpoint if necessary, provided that direct transports are estimated for the region shoreward of WB3. We therefore consider both the transports from the coast (Abaco) to WB2, which we refer to as the *western boundary wedge*, and from the coast to WB3, which we refer to as the *inner western boundary region*.

The mean meridional flow for the inner western boundary region over the length of the deployment is shown in Fig. 6, as derived from the above interpolation procedure. A coastally intensified northward flow occurs in the upper ocean with its core located vertically near 400 m. Maximum mean speeds near the coast reach approximately 0.4 m s^{-1}. This flow is a persistent feature of the regional mean circulation, and is consistent with earlier observations of the mean flow in this region over many years (Lee et al. 1990, 1996; Bryden et al. 2005). In the modern literature it is usually referred to as the Antilles Current (e.g., Lee et al. 1990), although it differs in important respects from the historical concept of a semicontinuous Antilles Current flowing from the tropics to the subtropics (e.g., Wüst 1924). Lee et al. (1996) attribute it to a recirculation of water in the western part of the North Atlantic subtropical gyre and partly to a more localized gyre or eddy centered just northeast of Abaco. Moreover, it is a subsurface-intensified current mainly involving subtropical mode water (18° Water), rather than a surface current as the historical notion of an Antilles Current implies. The surface currents close to Abaco overlying the strong northward core are almost zero in the mean. One can see in Figs. 3b,c that reversals to southward flow are common near the surface but are rare in the thermocline layer where the flow is persistently northward and at times can exceed 1 m s^{-1}. One can also see in Fig. 3 that the upper-ocean currents in the region shoreward of WB2 are highly correlated between moorings, implying that transports are well resolved in this region and that there is a fair degree of redundancy in the measurement array in case of failures.

Near a depth of 800 m the northward flow transitions abruptly to southward flow associated with the DWBC. Close to the western boundary an intense core of southward flow is found near 1200 m just at the top of the escarpment. This particular feature had not been well resolved by earlier studies that had sparser horizontal mooring separations (Lee et al. 1990); however, it had been occasionally observed in high-resolution shipboard surveys (Hacker et al. 1996; Johns et al. 1997). Flows in this feature frequently exceeded 0.4 m s^{-1}. Below this jet lies a region of weak or reversed flow at depths greater than ~1600 m, which, as noted above, is in a stagnant region behind upstream blocking ridges. It appears that the strong flow near 1200 m represents the uppermost part of the DWBC that is able to pass over these ridges to continue southward close to the western boundary, perhaps being intensified in the process. Farther offshore at mooring WB3, the core of the DWBC is found deeper, near 2000 m, consistent with previous results. From earlier studies, mooring WB3 is known to lie close to the mean core of the DWBC, or perhaps a few kilometers shoreward of it. Speeds here often reached 0.3–0.4 m s^{-1} through the depth range from 1200 to 4000 m and were persistently southward except for one notable reversal in November 2004, along with another brief reversal in late February 2005 (Fig. 3e).

The mean flow structure of Fig. 6 can be compared with the average flow observed by the three shipboard/lowered ADCP sections acquired during the period of the mooring array (Fig. 7). Although each cruise shows some differences, the average features compare well, including the thermocline-intensified Antilles Current, the upper DWBC core at 1200 m over the escarpment, and the deeper offshore DWBC core (note the different scales of the x axes in Figs. 6 and 7; Fig. 6 ends near the location of the DWBC core in Fig. 7). Evidence of the shielded region below 1600 m against the escarpment is also clear in Fig. 7. The DWBC is confined to within about 100 km from the western boundary in this average picture, which is also typical of previous results; however, the DWBC is known to occasionally meander farther offshore (Lee et al. 1996).

Transports derived from the moored current meter observations are shown in Fig. 8 for the regions shoreward of WB2 and shoreward of WB3, respectively. The region shoreward of WB2 is mainly influenced by the Antilles Current but also includes variability in the shallow portion of the DWBC over the escarpment. The region out to WB3, on the other hand, includes the greater part of the entire Antilles Current as well as the inshore part of the deeper DWBC. Two calculations are shown in Fig. 8: 1) the transports with WB2 included (until mid-December 2004) and 2) the transports with WB2 excluded and with currents interpolated between WB1 and WB3 including the fake topography of Fig. 6. The transport in the western boundary wedge inshore of WB2 varies from −4 to +7 Sv during the deployment and its mean value and variability are nearly identical between the two calculations; this we

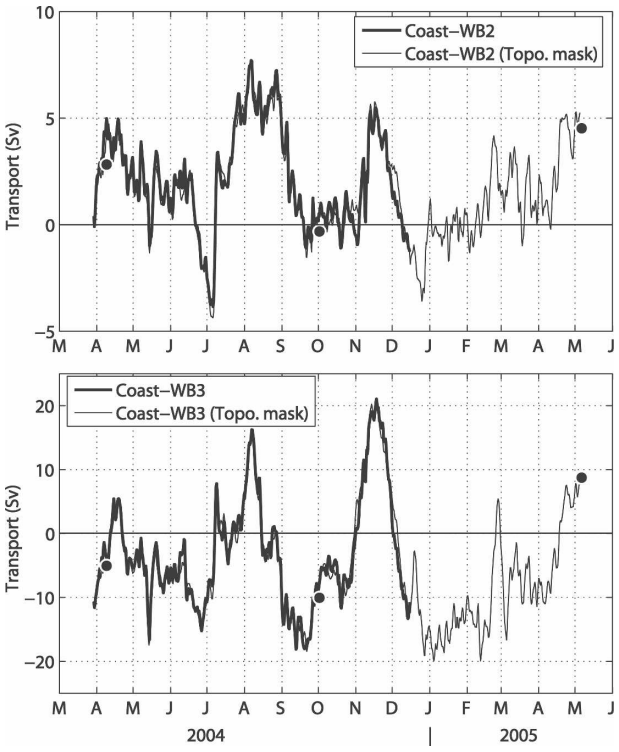

FIG. 8. Northward volume transports derived from the gridded current meter data for the region (top) from the coast to WB2 and (bottom) from the coast to WB3. The bold line includes deep current meter data on WB2; the light line shows the corresponding calculation when the deep data on WB2 is removed and replaced with the topographic mask displayed in Fig. 6. The dots show LADCP-derived transports at times of the cruise occupations.

take as evidence that the loss of data from WB2 during the latter part of the experiment is not a serious problem for the direct transport calculations. The transport inshore of WB3 has a significantly larger variability, from −20 to +20 Sv, but again shows excellent agreement between the two calculations. Comparisons with the transports estimated over these same regions from the three available LADCP sections also show very good agreement with the moored transport values, giving further confidence in the transport estimates. Accounting for the cross-correlations among the measured currents and allowing for measurement uncertainties we estimate that the moored transports for the region shoreward of WB2 are accurate to within ±0.5 Sv and those for the region shoreward of WB3 to within ±1.2 Sv (e.g., J05).

The vertical profile of the transport from the coast to WB3 is shown in Fig. 9, where the variability in the upper and lower layers can be more clearly discerned. The positive transport fluctuations are associated primarily with increasing northward flow in the upper ocean that have a typical time scale of several months. These fluctuations have been shown in previous records to be associated with baroclinic upper-ocean eddies propagating westward that modulate the mean northward Antilles Current (Lee et al. 1990, 1996; Halliwell et al. 1991). In the DWBC layer the most significant event during the record was the stoppage (and weak reversal) in the southward transport that occurred during November 2004. This event also contributed to the

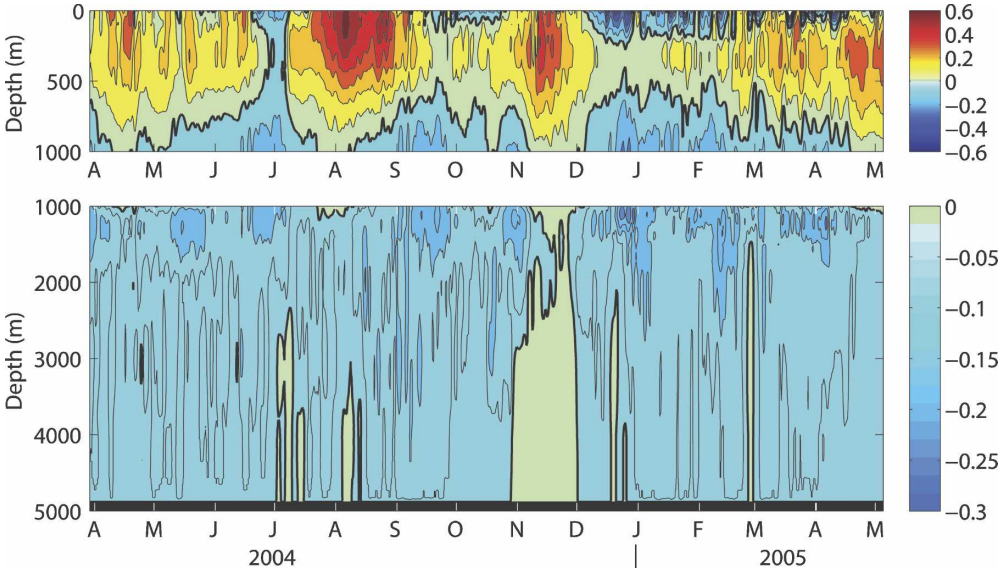

FIG. 9. Time series of the transport-per-unit-depth profile (10^5 m^2 s^{-1}) for the region extending from the coast to mooring WB3; the contour interval is decreased in the lower panel to better illustrate the deep variability. A notable reversal in the deep flow occurs during November 2004.

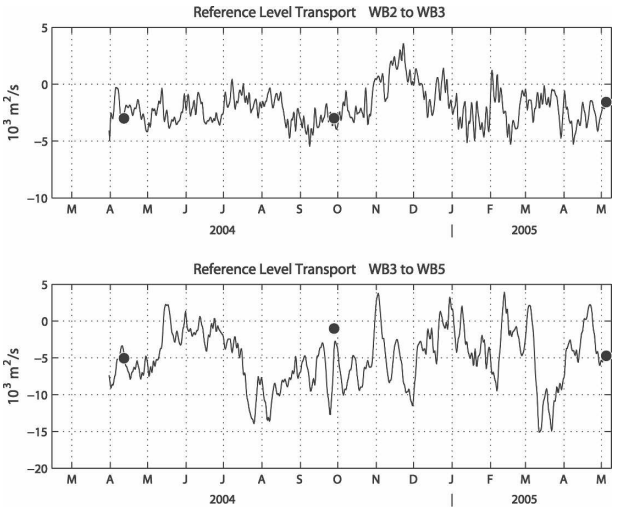

FIG. 10. Time series of the transport per unit depth derived from bottom pressure records referenced by LADCP measurements (dots) for the (top) WB2–WB3 mooring pair (reference level: 3800 dbar) and (bottom) WB3–WB5 mooring pair (reference level: 4800 dbar).

large northward pulse seen in the total transport at this time (Fig. 8b). The overall transport profile across this region typically shows a southward maximum near 1000–1500 m, owing to the shallow part of the DWBC flowing over the escarpment, even though the offshore DWBC core is closer to 2000 m.

b. *Transports across the extended western boundary layer*

To extend the transports across the full width of the western boundary layer to mooring WB5, we must compute indirect geostrophic transports for the WB3–WB5 region and combine them with the transports from the inner western boundary region. Unfortunately, with the lack of data from mooring WB4, it is not possible to break the transport down into a true western boundary layer contribution (which would include the entire region shoreward of WB4, spanning the typical limits of the Antilles Current and DWBC) and an "offshore" region where recirculation cells or other broad flows may exist. The western boundary layer contribution is, in fact, contained partly in the inner western boundary region discussed above and partly in the western region of the WB3–WB5 segment. Thus, it is not possible to isolate the western boundary transport from offshore transports in the present analysis.

The relative geostrophic transport profile for the region from WB3 to WB5 is computed as described above (section 3b) by differencing the dynamic height profiles

TABLE 1. Estimates of the transport-per-unit-depth reference value (V_0) for the WB2–WB3 and WB3–WB5 mooring pairs from the three project cruises, and the corresponding values used in the moored geostrophic transport calculations.

	V_0 (10^3 m^2 s^{-1})	
Cruise	WB2–WB3	WB3–WB5
April 2004	−2.46	−5.19
September 2004	−1.83	−1.53
May 2005	−1.66	−4.65
Average	−1.98 ± 0.42	−3.79 ± 1.97
Selected value	−1.98	−4.92*

* Average of April 2004 and May 2005 estimates.

at the mooring sites, and a time-varying reference value is added, which is determined from the bottom pressure gauges. The time series of the reference transport $V_{\text{ref}}(t) = V'_{\text{ref}}(t) + V_0$, where V_0 is the constant determined from the available shipboard LADCP measurements, is shown in Fig. 10. (We also show the comparable result for the WB2–WB3 mooring pair since we can compute an indirect geostrophic transport for this region as well.) Each of the LADCP sections produces an estimate of V_0 (Table 1), and the consistency of these estimates is a measure of how well the true reference value is determined.

Of the three estimates of V_0 for the WB3–WB5 mooring pair, two are in relatively good agreement (the April 2004 and May 2005 values, respectively; Table 1) while the third estimate is inconsistent with the others. Individual estimates of V_0 are expected to have relatively large uncertainty, since they depend on the accuracy of the relative geostrophic transports derived from the moorings and the LADCP velocity measurements, and on how well the LADCP section resolves the transport between the mooring pairs. Temporal variability in the flow that occurs during the occupation of the section can also cause errors. Particularly for the wide offshore region between WB3 and WB5, where the station spacing grows to as large as 50 km, the latter two issues can become important error sources. Still, the large discrepancy of the September 2004 V_0 estimate and the other two estimates is troubling, and despite considerable effort we have been unable to find any obvious data quality problems or processing errors in the cruise data that could explain it.

In comparison, the V_0 estimates for the WB2–WB3 mooring pair have a smaller spread, with an uncertainty of about ±20%. The moored geostrophic transport between WB2 and WB3 using the mean reference value from the three cruises shows a high correlation (r = 0.89) and a very similar vertical structure with that de-

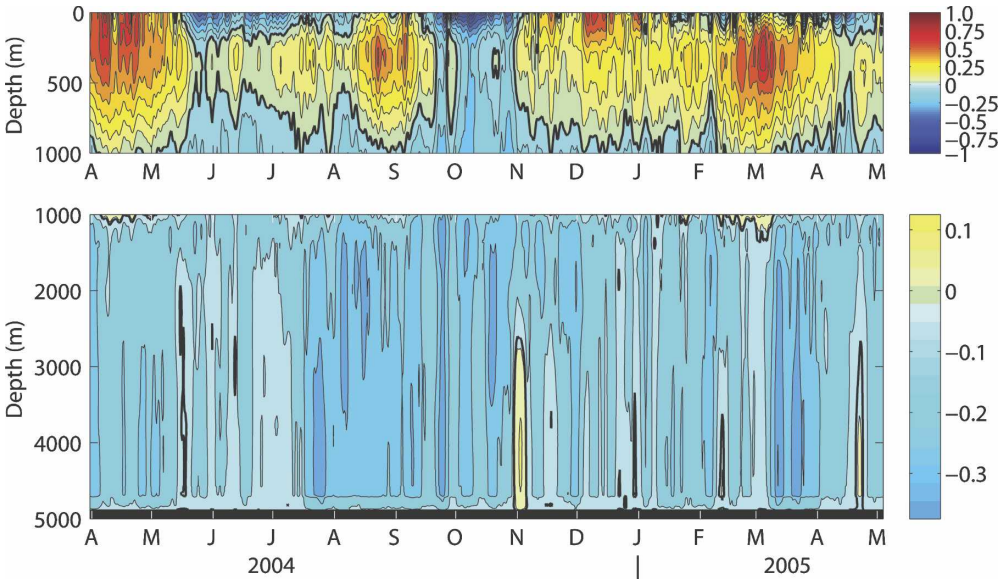

FIG. 11. Time series of the transport-per-unit-depth profile (10^5 m^2 s^{-1}) for the region extending from the coast to mooring WB5 at a distance of 500 km offshore.

rived from the direct current measurements (not shown), but the mean value of the geostrophic transport is smaller (less southward) by nearly 1.5 Sv. This suggests that the actual reference transport value may have been more negative (southward) than the mean estimate. For this reason we use the direct current meter transports for the inner western boundary region in the overall transport calculation, which (as shown in Fig. 8) agree well with the LADCP transports.

For our estimates of absolute transport in the offshore region between WB3 and WB5, we have chosen to use a value for V_0 that represents the average of the two (consistent) estimates and discard the third outlying estimate. Using this value (-4.9×10^3 m^2 s^{-1}; Table 1), instead of the mean value of the three estimates (-3.79×10^3 m^2 s^{-1}), results in the net southward transport in the WB3–WB5 region being larger by almost 5.0 Sv, and therefore it must be stated that the absolute transports in the offshore region are not yet well determined for this observing period. (For the interested reader we note that the RAPID–MOC strategy for referencing these transports involves the use of overlapped bottom pressure time series so that a continuous bottom pressure time series can be built up for each site without arbitrary offsets between individual deployment periods. Each LADCP section that is acquired across the array therefore provides an additional V_0 estimate that is applicable to the entire lifetime of the array. In this way a more statistically robust reference value can be obtained for the transports. This also means that the absolute transport values reported here may be revised in the future as more direct velocity sections become available.)

The time-varying transport profile across the full western boundary region, from Abaco to WB5 at a distance of ~500 km offshore, is shown in Fig. 11 after summing the results from the inner western boundary and offshore regions. The corresponding mean transport profiles for each region, and the net transport profile, are shown in Fig. 12.

The variability in the upper-ocean transport has the same characteristics as for the inner western boundary layer with dominant time scales of several months. Some of the events roughly coincide with each other (e.g., the events in April and August 2004; Figs. 9 and 11) but the phasing is different in other parts of the record. This reflects the different spatial integration volumes for the two regions and the fact that the extended western boundary layer is probably less influenced by individual eddies than the near-boundary region. The width of the extended western boundary layer (500 km) is about twice the typical wavelengths (230–340 km) of the westward propagating features found in the region (Lee et al. 1996). Thus, the transports over the extended western boundary layer should act as a filter on the local mesoscale variability to a degree, provided that the eddy energy decreases to the east, which is the case (Zantopp et al. 1993, 1996).

In the deeper part of the water column the transport profile no longer shows the persistent upper DWBC core at ~1200 m found in the inner western boundary region but, instead, a transport maximum that can vary

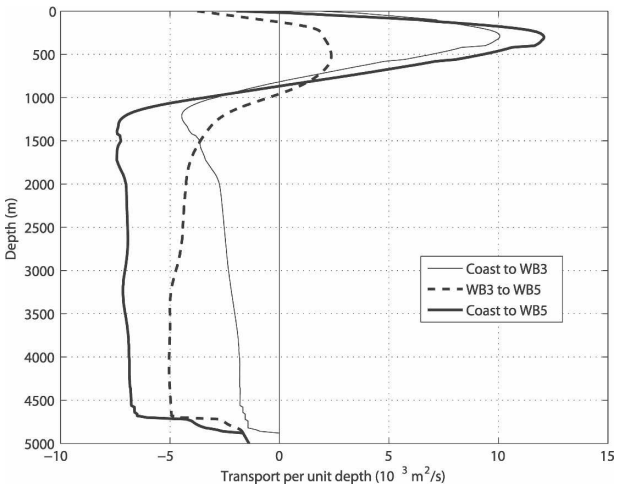

FIG. 12. Mean transport profile for the whole western boundary layer (coast to WB5) and its contributions from the near-boundary (coast to WB3) and offshore (WB3 to WB5) areas.

anywhere between 2000 and 4000 m. Several reversals occur in the deep southward flow below about 3000 m during the record, most notably in early November 2004, but also briefly in May and December 2004 and again in February and April 2005.

In the mean transport profiles (Fig. 12) it is clear that the majority of the net northward flow across the full western boundary region is contained in the inner western boundary region. The offshore region still has a weak net northward flow in the thermocline, but its contribution is only about one-fifth of the net northward flow. The total northward transport in the upper 1000 m is 6.0 Sv (Table 2), which is very similar to earlier estimates of 5.0 ± 1.8 Sv for the mean Antilles Current off Abaco (Lee et al. 1996). In the deep water the mean inner western boundary profile again shows the maximum southward flow near 1200 m, but in the offshore region it reaches its maximum below 3000 m. The net transport profile for the entire western boundary layer is almost uniform between 1200 and 4700 m, indicating no particular core depth for the southward DWBC flow when spatially integrated across this region. The total deep southward transport over the period of the deployment is −26.5 Sv (Table 2), which, as a consequence of the uniform vertical structure, is nearly equally divided between layers associated with upper North Atlantic Deep Water (UNADW: ~1000–3000 m, −13.9 Sv) and lower North Atlantic Deep Water (LNADW: ~3000–5000 m, −12.6 Sv). We reiterate that we are not able to determine from the present analysis the contribution of the DWBC itself to these transports versus the compensation by offshore recirculation.

TABLE 2. Mean volume transports for the western boundary region, cumulative from Bahamas escarpment to 72°W, for the present study compared with Bryden et al. (2005).

Layer	Transport (Sv)	
	This study	Bryden et al. (2005)
0–1000 m	6.0	−0.1
1000–3000 m	−13.9	−12.9
3000–5000 m	−12.6	−11.3
1000–5000 m	−26.5	−24.2

Time series of the net transports across the extended western boundary layer, for the upper 1000 m and below 1000 m, are shown in Fig. 13. Very large fluctuations occur in both upper and lower layers with transports above 1000 m varying between −15 and +25 Sv and deep transports varying between −60 and +3 Sv. Transport comparisons derived from the shipboard/lowered ADCP data show good agreement for all but the deep transport during the September 2004 cruise, which was the root of the problem in the referencing issue, as noted above. Similarly large transport fluctuations were observed by Meinen et al. (2006) from an array of inverted echo sounders and bottom pressure gauges deployed across the same region from September 2004 to September 2005. Their transport fluctuations calculated over an equivalent deep layer (800–4800 m, their Fig. 3) agree very closely ($r = 0.88$) with those in Fig. 13 for the overlapping period of the time series (September 2004–April 2005). However, they obtained a considerably smaller mean southward deep transport across this region (−11 Sv) based on initial comparisons with (preliminary) LADCP data.

It is clear from examining Fig. 11, particularly in the deep water, that a large part of the variability in the deep transports on time scales of several days to weeks is due to fluctuations that are nearly barotropic. These fluctuations are sufficiently strong that they can lead to reversals of the net southward flow across this region, even with its relatively large mean value of −26 Sv. Similarly large fluctuations have been observed previously in this area (Lee et al. 1990, 1996). We will not go into details here on the nature of these barotropic fluctuations except to say that they appear to have very large zonal spatial scales, O(2000 km) or greater, based on cross-spectral analysis of the bottom pressure records (not shown); this is also obvious from their high correlation, see Fig. 5), and fast zonal (westward) propagation speeds of 1–2 m s^{-1}. They most likely represent transient basin modes or other atmospherically forced barotropic Rossby waves. They may also be partly related to the nonequilibrium oceanic response to the long-period tides, in particular the fortnightly

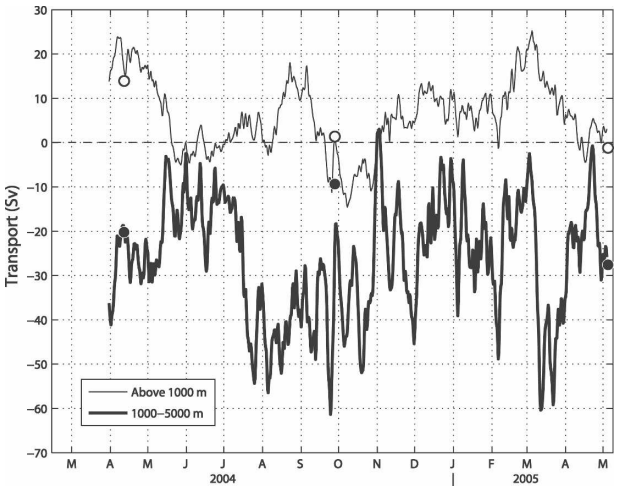

FIG. 13. Northward volume transport between Abaco Island and mooring WB5, spanning a distance of 500 km from the western boundary. The light line shows the transport above 1000 m; bold line shows the net transport below 1000 m. Transports derived from LADCP sections are superimposed (open circles for the upper 1000 m, solid circles for the deep transport).

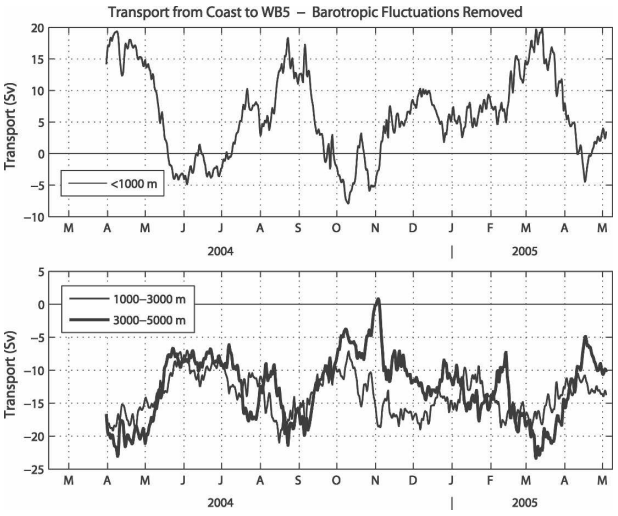

FIG. 14. Northward volume transport over the whole western boundary layer after removing barotropic transport fluctuations (top) for the top 1000 m and (bottom) for the Upper NADW (1000–3000 m) and Lower NADW (3000–5000 m) layers.

(M_f) tide, which involves large-scale geostrophic flows (Egbert and Ray 2003). Although interesting in their own right, for our purposes we consider these fluctuations to represent high-frequency noise on the baroclinic, and ultimately lower-frequency, signals that are of most interest in the context of MOC variability.

c. *Internal variability of the DWBC*

To reveal more clearly the internal variability of the western boundary flow, the barotropic signal is removed from the transports in Fig. 13 and the result is shown in Fig. 14, where the total deep transport is now broken up into the upper and lower NADW layers. This is done by removing, at each time step, the *deviation* of the vertically averaged transport per unit depth from its time mean value [i.e., $\langle V\,(t)\rangle - \langle V^*\rangle$], where angle brackets represent vertical averaging and the asterisk represents a time average. Thus, the time-mean barotropic flow is retained (and hence time mean transports of the upper and lower layers), while the fluctuations in barotropic flow are filtered.

Much of the high frequency variability is now gone from the time series, which is especially evident in the deep transports. The remaining baroclinic variations highlight changes in the transport of the DWBC relative to its time mean value that are not related to barotropic fluctuations and, in particular, it illustrates changes in the partitioning of the deep transport among the UNADW and LNADW layers. (Prior to removing the barotropic fluctuations the visual impression was simply that these two layers covaried throughout the time series.) The deep layer transports still covary to a degree but there are significant differences during parts of the record, particularly during October–December 2004 when the LNADW layer transport weakens relative to the UNADW layer; the LNADW layer actually shuts off briefly in early November. This shutoff also occurs for the total transport below 1000 m, in Fig. 13, but it is now clear that that is partly an effect of the barotropic variability and that the UNADW transport is not much different from its long-term mean value during this event. A number of other such "near shutoffs" occur (Fig. 13) for the total deep transport, but all of these are primarily due to the barotropic fluctuations, and none have the character of the November 2004 event (except for weaker events in February and April 2005, which have a hint of this behavior).

The November 2004 event clearly stands out as an interesting and unique event in the record. The changes in relative transports of the UNADW and LNADW layers imply large changes in the deep shear structure of the DWBC and, therefore, in the slope of the deep density surfaces across the western boundary layer. In the mean, the shear between the northward-flowing Antilles Current and the DWBC requires an upward slope of the isopycnals toward the western boundary at the top of the DWBC and a deepening toward the western boundary at the base of the DWBC (if there is a middepth DWBC core, such as occurs near the western boundary). In Fig. 4 this can be seen in the difference in isotherm depths between moorings WB2 and WB3, which closely correspond to the density surfaces in deep

water. Near the top of the DWBC the isotherms are shallower at the inshore site (e.g., 5°C), whereas below the DWBC core they are typically deeper (3°C near 2500 m). Thus, there is a stratification minimum (potential vorticity minimum) associated with the core of the DWBC near the western boundary that derives from its formation source in the subpolar North Atlantic, a classical feature of the DWBC.

During the event of November 2004, the isotherms at the depth approximately separating UNADW from LNADW (2500–3500 m) are seen to dip markedly, especially at site WB2 right near the escarpment. The 3°C isotherm dipped by almost 500 m during this event and was nearly 200 m deeper than at any other time in the record. Other events of similar nature took place during the record (e.g., February 2005), but the November event was characterized by a particularly large amplitude and coherence of the isotherm displacements through this layer. This produced a large southward shear in this layer (a decreasing southward flow with depth), effectively shutting off the southward flow of the lower DWBC. We speculate that this process must reflect a boundary wave phenomenon, amounting essentially to an internal Kelvin-like disturbance of the deep interfaces between the UNADW and LNADW propagating down the western boundary. Although this event is unique within this record, it seems likely that such events happen at other times and are likely part of the normal variability of the DWBC at this location, or other locations. Examining the records from the decade-long historical current meter dataset off Abaco (Lee et al. 1990, 1996; J05), we find evidence for two other events with similar characteristics, although those data are typically confined closer to the coast and may not necessarily reflect integrated changes across the whole DWBC. This suggests that the event observed in November 2004 is not unique, but that such events are not particularly frequent either.

5. Discussion

The measurements presented in this paper are part of a larger effort to determine the strength of the meridional overturning circulation in the midlatitude North Atlantic and to monitor it continuously for a long enough period to determine its variability characteristics. Long-term monitoring of the MOC via some form of semioperational system will be important for understanding the role of MOC variability in climate variability and future climate change. Key components of the MOC occur in the western boundary layer off the Bahamas, and we show here how these components can be monitored with current meters and dynamic height moorings.

The data from this 1-yr experiment are not sufficient to determine the mean flows and transports across this region with statistical certainty, but we can compare the results with other long-term estimates to assess their representativeness. Bryden et al. (2005), using all available current measurements from the historical Abaco current meter arrays in this region between 1986 and 1997, constructed a mean section of meridional flow extending from the boundary to near 71°W, or approximately 600 km offshore. The resulting picture shows a mean southward DWBC confined within 150 km of the western boundary and an overlying Antilles Current, similar to that shown in Fig. 7, except that the mean DWBC in Bryden et al. (2005, their Fig. 3) is broader, a feature related to periodic offshore meandering of the DWBC (e.g., Lee et al. 1996). The mean southward transport of the DWBC over this region was calculated by Bryden et al. to be -34.6 ± 4 Sv, with an overlying Antilles Current transport of 5.1 Sv (no error estimate given). Offshore of the DWBC (Fig. 4 of Bryden et al.) the flow is characterized by broad northward recirculation at depths from 1000 to 3500 m, concentrated between 75° and 72°W, with some bands of deeper southward flow near the bottom. This picture is consistent with other descriptions of the offshore flow developed from individual shipboard surveys (Johns et al. 1997), float data (Leaman and Vertes 1996), and earlier current meter data (Lee et al. 1996). Summing the western boundary and offshore regions, Bryden et al. found a net southward transport below 1000 m of -24.2 Sv, suggesting a deep offshore recirculation $O(10$ Sv). Bryden et al. note that this value is comparable to estimates of 21–23 Sv for the net southward deep transport across 25°N based on hydrographic sections (Lavin et al. 1998).

In Fig. 15 we compare the mean transport profile for the extended western boundary layer (from our Fig. 12) with the corresponding results from Bryden et al. (2005) for the mean current meter section extending to 71°W (their Fig. 6). The two section lengths are not identical, the latter extending 100 km farther offshore. The estimate of -26.5 Sv that we obtain for the net southward deep transport compares favorably with that of Bryden et al. (Table 2). The only notable difference in the deep transport profile is the local minimum near 3000 m in Bryden et al. separating two cores of stronger southward flow near 2000 and 4000–4500 m, which is not present in our results. The most significant difference is in the upper ocean where neither the magnitude nor the structure of the transport above 1000 m agrees. In the Bryden et al. compilation a relatively strong southward flow occurs in the offshore region between 73° and 71°W at depths of 300–800 m, which compen-

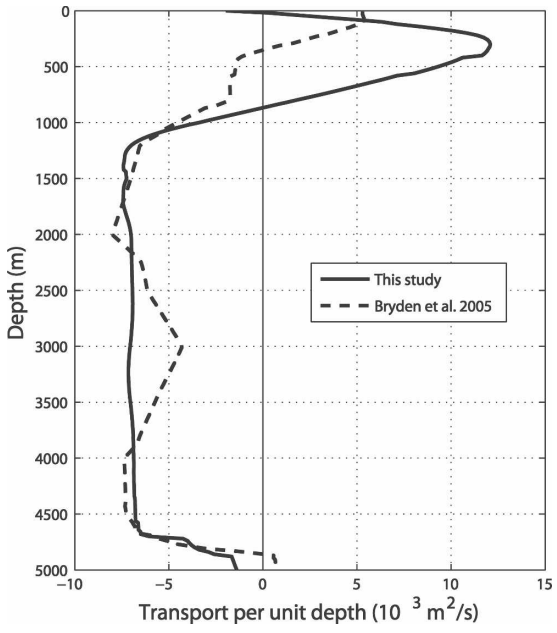

FIG. 15. Mean transport profile from the coast to WB5 for the period March 2004–May 2005 (from Fig. 12) compared with a similar estimate derived from long-term historical current meter data by Bryden et al. (2005).

sates the northward Antilles Current closer to shore and leads to a near-zero net transport across the full region (Table 2). Whether this is a true inconsistency of the results or is related to the much different averaging periods of the two estimates is unclear. As Bryden et al. note, there is still a potential for large error in their offshore transport estimates because of the large separation (100 km or more) between the moorings, even if the long-term mean currents obtained at the measurement sites are significant (and some are only marginally so). The consistency of the deep transports between the two studies suggests that the net DWBC flow (including offshore recirculation) measured during the 2004–05 period is representative of the long-term average, however.

The analysis of these new measurements revealed one new feature of the mean flow that had not been well resolved before—the intense upper core of the DWBC flowing over the top of the Bahamas escarpment near 1200 m. While it is not a very important feature in the overall transport picture, it is a component that likely had been missed or underestimated in earlier studies. In terms of the variability, the main feature of interest in the DWBC, apart from its large overall variability, was the occurrence of a temporary shutoff in the lower part of the DWBC, which appears to be a relatively rare event. We are able to show from the extended western boundary array data that this cannot be attributed to a meander of the DWBC and, also, that it is not simply a consequence of the large background barotropic variability in the region but, indeed, reflects a real and significant internal change in the DWBC structure. It is not clear what forced this variation, and it is probably not very likely that it is directly linked to a water-mass formation event in the source region of the DWBC. However, what is interesting about this event is that it may be dynamically representative of the kind of signal that would be associated with a change in the transport or structure of the DWBC on longer time scales (e.g., Döscher et al. 1994). As such, it will be interesting to see if this signal can be traced in other contemporaneous data or observations in the North Atlantic—a topic for further investigation.

The determination of absolute transports with the methodology employed here is a rather involved procedure owing to the need to reference the geostrophic transports with additional direct velocity measurements and, as we show here, it can lead to significant errors in absolute transports. These errors should decrease with time as longer continuous records are obtained and more direct velocity sections are acquired across the measurement array. However, it is important to stress that the determination of *transport variability* via dynamic height moorings is immune to this referencing problem and has errors that are no worse than typically can be obtained with an array of "resolving" current meter moorings (J05). In this sense the estimation of transport variability from widely spaced dynamic height moorings is relatively easy, while the determination of absolute transports is more difficult. It should also be noted that the estimation of the transbasin MOC from the RAPID program array does not depend on this referencing procedure in any way and, in fact, does not require the availability of bottom pressure measurements (Hirschi et al. 2003). To estimate the basinwide MOC, only the geostrophic shear needs to be estimated from the deep water moorings, which is then combined with direct measurements in boundary regions (Florida Current, western/eastern boundary "wedges"), Ekman transport estimates, and an overall zero mass flux constraint (Kanzow et al. 2007; Cunningham et al. 2007). However, an understanding of the barotropic motions is valuable, as it can provide insight to the mechanisms by which the MOC varies and by which mass balance is achieved across the basin (Kanzow et al. 2007).

Other dynamical processes that the extended RAPID–MOC western boundary array should help to resolve include the large-scale response of the Atlantic Ocean to time-variable wind forcing. Especially at seasonal time scales, a large transport variation is expected in the western boundary layer as a result of the quasi-

stationary barotropic response of the basin to interior wind stress curl forcing (Anderson and Corry 1985; Lee et al. 1996). This signal is expected to have an amplitude of approximately 13 Sv (Anderson and Corry 1985) with maximum northward transport anomaly in winter (January) and maximum southward transport anomaly in fall (October). A hint of this cycle is perhaps visible in Fig. 12 (in the deep transports) but, as Lee et al. (1996) demonstrated, it takes several years of data to be able to discern such a signal from the energetic barotropic background. In any case, the use of naturally integrating geostrophic measurements, including continuous bottom pressure measurements, over such a wide boundary layer section should be advantageous in attempting to resolve these motions.

6. Summary

Our objectives in this study have been twofold: (i) to establish the methodology for obtaining direct transports in the "inner" western boundary region off the Bahamas for use in a basinwide estimate of the MOC strength and variability (Cunningham et al. 2007) and (ii) to investigate the variability in the Antilles Current–DWBC system over a larger western boundary region extending from the Bahamas to 500 km offshore.

The main results are summarized as follows:

From the closely spaced current meter observations near the western boundary we are able to determine the time-varying western boundary layer transports to within ±0.5 Sv over the Bahamas escarpment inshore of 3800 m, where instantaneous transports vary from −4 to 7 Sv. These transports provide one of four principal components needed to monitor the time-varying strength and structure of the MOC at this latitude, the other three being the Florida Current transport, the midocean geostrophic transport, and the basinwide Ekman transport (Cunningham et al. 2007).

The transport of the upper-ocean Antilles Current off Abaco, Bahamas, is 6.0 Sv during the period of these observations (March 2004–May 2005), consistent with earlier estimates derived from long-term current meter arrays deployed in this same region within 100 km of the western boundary (Lee et al. 1996; Bryden et al. 2005). However, unlike Bryden et al., we find no evidence for significant southward recirculation in the upper ocean in the offshore region (~100–500 km offshore) that compensates the northward transport along the western boundary.

The mean southward transport of the DWBC over the extended western boundary layer (Abaco to 500 km offshore), inclusive of northward recirculation, is −26.5 Sv during the period of observation and is divided nearly equally between the upper North Atlantic Deep Water (1000–3000 m; −13.9 Sv) and lower North Atlantic Deep Water (3000–5000 m; −12.6 Sv) layers. These transports agree well with corresponding estimates (−24.2, −12.9, and −11.3 Sv, respectively, for the total, upper, and lower NADW layers) derived from historical current meter observations (Bryden et al. 2005).

Both the current meter data and closely spaced lowered-ADCP sections collected during the period of observations reveal a secondary "upper" core of the DWBC flowing close to the western boundary over the top of the Bahamas escarpment near ~1200 m depth, a feature that had not been well resolved in earlier investigations.

Transport fluctuations within the Abaco western boundary layer are extremely large (from −15 to 25 Sv in the upper 1000 m and −60 to 3 Sv in the layers below 1000 m) and are dominated by nearly barotropic fluctuations. The nature of these barotropic fluctuations, though known from previous studies (Lee et al. 1996; Meinen et al. 2006), requires further study in terms of their spatial scales and forcing mechanisms.

Superimposed on these large barotropic fluctuations, significant internal changes in the structure of the DWBC are revealed by the observations, including one extreme event in which the lower NADW layer of the DWBC stopped flowing southward entirely for a brief (~10 day) period. It is shown in Cunningham et al. (2007) that this corresponded to a similar brief shutoff in the lower NADW flow across the entire transatlantic section. Thus, the vertical structure of the DWBC, as well as that across the entire basin, is subject to significant short-term variability by processes acting at the western boundary.

As of this writing the RAPID–MOC array has been deployed for 2.5 years, with the second year of data now in analysis. With presently secured funding the measurements will continue for four years, until spring 2008, and plans are being developed to extend the program though 2014 so that a full decade of DWBC and MOC variability observations can be obtained.

Acknowledgments. This research was supported by the U.S. National Science Foundation under Award OCE0241438, by the U.K. RAPID Programme (RAPID Grant NER/T/S/2002/00481), and by the U.S.

National Oceanic and Atmospheric Administration, as part of its Western Boundary Time Series Program. The mooring deployment and recovery operations were skillfully carried out by the University of Miami Ocean Technology Group and the U.K. Natural Environment Research Council UKORS mooring group. The authors thank the captains and crews of the RRS *Discovery*, R/V *Knorr*, and R/V *Ronald H. Brown* for their dedication and capable assistance in the mooring cruises and shipboard data acquisition activities.

REFERENCES

Akima, H., 1970: A new method of interpolation and smooth curve fitting based on local procedures. *J. Assoc. Comput. Mach.,* **17,** 589–602.

Anderson, D. L. T., and R. A. Corry, 1985: Seasonal transport variations in the Florida Straits: A model study. *J. Phys. Oceanogr.,* **15,** 773–786.

Bryden, H. L., W. E. Johns, and P. M. Saunders, 2005: Deep western boundary current east of Abaco: Mean structure and transport. *J. Mar. Res.,* **63,** 35–57.

Cunningham, S. A., and Coauthors, 2007: Temporal variability of the Atlantic meridional overturning circulation at 26.5°N. *Science,* **317,** 935–938.

Döscher, R., C. W. Böning, and P. Herrmann, 1994: Response of circulation and heat transport in the North Atlantic to changes in thermohaline forcing in northern latitudes: A model study. *J. Phys. Oceanogr.,* **24,** 2306–2320.

Egbert, G. D., and R. D. Ray, 2003: Deviation of long-period tides from equilibrium: Kinematics and geostrophy. *J. Phys. Oceanogr.,* **33,** 822–839.

Fillenbaum, E. R., T. N. Lee, W. E. Johns, and R. Zantopp, 1997: Meridional heat transport variability at 26.5°N in the North Atlantic. *J. Phys. Oceanogr.,* **27,** 153–174.

Ganachaud, A., and C. Wunsch, 2000: Improved estimates of global ocean circulation, heat transport and mixing from hydrographic data. *Nature,* **408,** 453–457.

Hacker, P., E. Firing, W. D. Wilson, and R. Molinari, 1996: Direct observations of the current structure east of the Bahamas. *Geophys. Res. Lett.,* **23** (10), 1127–1130.

Hall, M. M., and H. L. Bryden, 1982: Direct estimates and mechanisms of ocean heat transport. *Deep-Sea Res.,* **29,** 339–359.

Halliwell, G. R., Jr., P. Cornillon, and D. A. Byrne, 1991: Westward-propagating SST anomaly features in the Sargasso Sea, 1982–88. *J. Phys. Oceanogr.,* **21,** 635–649.

Hirschi, J., J. Baehr, J. Marotzke, J. Stark, S. Cunningham, and J.-O. Beismann, 2003: A monitoring design for the Atlantic meridional overturning circulation. *Geophys. Res. Lett.,* **30,** 1413, doi:10.1029/2002GL016776.

Johns, E., R. A. Fine, and R. L. Molinari, 1997: Deep flow along the western boundary south of the Blake Bahama Outer Ridge. *J. Phys. Oceanogr.,* **27,** 2187–2208.

Johns, W. E., R. Zantopp, T. N. Lee, D. Zhang, C.-T. Liu, and Y. Yang, 2001: The Kuroshio east of Taiwan: Moored transport observations from the WOCE PCM-1 array. *J. Phys. Oceanogr.,* **31,** 1031–1053.

——, ——, and T. Kanzow, 2005: Estimating ocean transports with dynamic height moorings: An application in the Atlantic deep western boundary current. *Deep-Sea Res. I,* **52,** 1542–1567.

Kanzow, T., U. Send, W. Zenk, A. D. Chave, and M. Rhein, 2006: Monitoring the integrated deep meridional flow in the tropical North Atlantic: Long-term performance of a geostrophic array. *Deep-Sea Res. I,* **53,** 528–546.

——, and Coauthors, 2007: Observed flow compensation associated with the MOC at 26.5°N in the Atlantic. *Science,* **317,** 938–941.

Lavin, A., H. L. Bryden, and G. Parrilla, 1998: Meridional transport and heat flux variations in the subtropical North Atlantic. *Global Atmos. Ocean Syst.,* **6,** 269–293.

Leaman, K. D., and P. S. Vertes, 1996: Topographic influences on recirculation in the deep western boundary current: Results from RAFOS float trajectories between the Blake–Bahama Outer Ridge and the San Salvador "gate." *J. Phys. Oceanogr.,* **26,** 941–961.

Lee, T. N., W. E. Johns, R. Zantopp, and F. Schott, 1990: Western boundary current structure and variability east of Abaco, Bahamas at 26.5°N. *J. Phys. Oceanogr.,* **20,** 446–466.

——, ——, ——, and E. R. Fillenbaum, 1996: Moored observations of western boundary current variability and thermohaline circulation at 26.5°N in the subtropical North Atlantic. *J. Phys. Oceanogr.,* **26,** 962–963.

Lumpkin, R., and K. Speer, 2003: Large-scale vertical and horizontal circulation in the North Atlantic Ocean. *J. Phys. Oceanogr.,* **33,** 1902–1920.

Meinen, C. S., M. O. Baringer, and S. L. Garzoli, 2006: Variability in Deep Western Boundary Current transports: Preliminary results from 26.5°N in the Atlantic. *Geophys. Res. Lett.,* **33,** L17610, doi:10.1029/2006GL026965.

Schmitz, W. J., Jr., and M. S. McCartney, 1993: On the North Atlantic circulation. *Rev. Geophys.,* **31,** 29–50.

Visbeck, M., 2002: Deep velocity profiling using lowered acoustic Doppler current profilers: Bottom track and inverse solutions. *J. Atmos. Oceanic Technol.,* **19,** 794–807.

Watts, D. R., and H. Kontoyiannis, 1990: Deep-ocean bottom pressure measurement: Drift removal and performance. *J. Atmos. Oceanic Technol.,* **7,** 296–306.

Whitworth, T., III, 1983: Monitoring the transport of the Antarctic Circumpolar Current at Drake Passage. *J. Phys. Oceanogr.,* **13,** 2045–2057.

Wüst, G., 1924: Florida- und Antillenstrom. Berlin U., Institut für Meereskunde, Veröff., N. F., A. Geogr.-naturwiss, Reihe, Heft 12, 48 pp.

Zantopp, R. J., T. N. Lee, and W. E. Johns, 1993: Moored current meter observations east of Abaco, the Bahamas (WATTS Array). University of Miami RSMAS Tech. Rep. 93-006, 77 pp.

——, ——, and ——, 1996: Moored current meter observations east of Abaco, the Bahamas (ACCP-1 Array). University of Miami RSMAS Tech. Rep. 96-001, 80 pp.